

Original Article

Effects of the histamine H₁ receptor antagonist hydroxyzine on hERG K⁺ channels and cardiac action potential duration

Byung Hoon LEE^{1,2}, Seung Ho LEE³, Daehyun CHU⁴, Jin Won HYUN⁵, Han CHOE^{4,*}, Bok Hee CHOI^{3,*}, Su-Hyun JO^{1,*}

¹Department of Physiology, Institute of Bioscience and Biotechnology, Kangwon National University School of Medicine, Chuncheon 200–701, Korea; ²Department of Radiology, Ilsan Paik Hospital, Inje University School of Medicine, Goyang 411–706, Korea;

³Department of Pharmacology, Institute for Medical Sciences, Chonbuk National University Medical School, Jeonju, Jeonbuk 561–180, Korea; ⁴Department of Physiology, Bio-Medical Institute of Technology, University of Ulsan College of Medicine, Seoul 138–736, Korea;

⁵Department of Biochemistry, School of Medicine, Jeju National University, Jeju 690–756, Korea

Aim: To investigate the effects of hydroxyzine on human *ether-a-go-go*-related gene (hERG) channels to determine the electrophysiological basis for its proarrhythmic effects.

Methods: hERG channels were expressed in *Xenopus* oocytes and HEK293 cells, and the effects of hydroxyzine on the channels were examined using two-microelectrode voltage-clamp and patch-clamp techniques, respectively. The effects of hydroxyzine on action potential duration were examined in guinea pig ventricular myocytes using current clamp.

Results: Hydroxyzine (0.2 and 2 μmol/L) significantly increased the action potential duration at 90% repolarization (APD₉₀) in both concentration- and time-dependent manners. Hydroxyzine (0.03–3 μmol/L) blocked both the steady-state and tail hERG currents. The block was voltage-dependent, and the values of IC₅₀ for blocking the steady-state and tail currents at +20 mV was 0.18±0.02 μmol/L and 0.16±0.01 μmol/L, respectively, in HEK293 cells. Hydroxyzine (5 μmol/L) affected both the activated and the inactivated states of the channels, but not the closed state. The S6 domain mutation Y652A attenuated the blocking of hERG current by ~6-fold.

Conclusion: The results suggest that hydroxyzine could block hERG channels and prolong APD. The tyrosine at position 652 in the channel may be responsible for the proarrhythmic effects of hydroxyzine.

Keywords: histamine antagonists; hydroxyzine; cardiomyocytes; hERG channels; K⁺ channel; proarrhythmic effects

Acta Pharmacologica Sinica (2011) 32: 1128–1137; doi: 10.1038/aps.2011.66

Introduction

The cardiac action potential is composed of five distinct phases that are designated phases 0–4^[1]. The precise shape of the action potential is determined by the coordinated activity of many various ion channels. The action potential is also responsible for the propagation of excitation information from cell to cell and allows the heart to function as a syncytium. The initial upstroke (phase 0) is due to inward Na⁺ current (I_{Na}) through fast-activating voltage-gated Na⁺ channels. The initial rapid repolarization phase (phase 1) results from rapid voltage-dependent inactivation of the fast inward I_{Na} and the

activation of a transient outward current (I_{to}) and the ultra-rapid components of the delayed rectifier K⁺ current (I_{Kur}). During phase 2, inward depolarizing currents through Na⁺ and L-type Ca²⁺ channels are balanced by the various components of the delayed rectifier K⁺ current, such as I_{Kur}, the rapidly activating delayed rectifier K⁺ current (I_{Kr}), and the slowly activating delayed rectifier K⁺ current (I_{Ks}). The terminal phase 3 of repolarization is due to increasing conductance of the channels that carry I_{Kr}, I_{Ksr} and inwardly rectifying K⁺ currents (I_{Kir})^[2].

Several ion currents such as inward Na⁺ and Ca²⁺ currents and outward K⁺ currents contribute to the duration of the cardiac action potential. However, the most common mechanism of delayed repolarization—which results in a prolonged QT interval—is by blocking one or more outward K⁺ currents^[3]. Among the various cardiac K⁺ currents, I_{Kr} is the most critical current for terminating the cardiac action potential, and this

* To whom correspondence should be addressed.

E-mail suhyunjo@kangwon.ac.kr (Su-Hyun JO);

bhchoi@jbnu.ac.kr (Bok Hee CHOI);

hchoe@amc.seoul.kr (Han CHOE).

Received 2011-01-13 Accepted 2011-04-22

current determines the shape of the repolarization phase^[4]. The pore-forming α subunit of the I_{Kr} channel is the human *ether-a-go-go*-related gene (hERG) protein. In the heart, I_{Kr} contributes prominently to terminal repolarization in humans^[5].

The mechanism that is often proposed for drug-induced QT interval prolongation is the direct block of hERG channels^[6]. Thus, the inhibition of K^+ currents through hERG can result in a prolongation of the cardiac action potential duration, *torsades de pointes* and sudden cardiac death. Long QT syndrome is characterized by a prolongation of the QT interval on the electrocardiogram. This lengthening of the QT interval usually indicates delayed repolarization of the action potential in ventricular myocytes^[3]. In addition, QT interval prolongation is a risk factor for *torsades de pointes*, a potentially fatal form of ventricular arrhythmia.

Hydroxyzine is a first generation sedating antihistamine commonly used for treating a variety of conditions. It is one of the most potent histamine 1 (H_1) receptor antagonists^[7]. Abnormal ventricular repolarization^[8, 9] and sinus tachycardia^[9, 10] have been shown to underlie the cardiac toxicity that can occur with hydroxyzine use. The second generation antihistamines terfenadine and astemizole produce cardiac toxicity primarily in the form of an increased risk for *torsades de pointes*^[7]. Both terfenadine and astemizole are H_1 -receptor antagonists that also block hERG channels^[11].

The purpose of this study was to investigate the acute effects of hydroxyzine on both cardiac action potentials in guinea pig ventricular myocytes and recombinant hERG channels expressed in *Xenopus laevis* oocytes and HEK cells to determine the electrophysiological basis for hydroxyzine's proarrhythmic effects. In addition, we examined the molecular basis of this block using a mutant (Y652A) hERG channel. Finally, a virtual docking simulation was used to propose a hydroxyzine-blocking mode of the hERG channel using the KvAP channel structure as a template.

Materials and methods

Ventricular myocyte isolation

Single ventricular myocytes were isolated from guinea pig hearts using a method that was described previously^[12]. In brief, guinea pigs (300–500 g) were anesthetized with pentobarbital (~50 mg/kg, ip) and the heart was quickly excised. The heart was retrogradely perfused sequentially at 37 °C with a 750 $\mu\text{mol/L}$ Ca^{2+} solution, a Ca^{2+} -free solution, and one containing 150 $\mu\text{mol/L}$ Ca^{2+} , collagenase type I and protease type XIV. The heart was then flushed with a 150 $\mu\text{mol/L}$ Ca^{2+} solution. The ventricles were removed and chopped into small pieces, which were then shaken in a flask containing a 150 $\mu\text{mol/L}$ Ca^{2+} solution. The cells in suspension were then allowed to sediment, and the supernatant was replaced with a 500 $\mu\text{mol/L}$ Ca^{2+} solution. The cells were kept at room temperature. These experiments were conducted with the approval of the Research Guidelines of Kangwon National University IACUC.

Solutions and action potential recordings from myocytes

Myocytes in the experimental chamber were continuously superfused at room temperature (24–26 °C) with Tyrode's solution containing 10 mmol/L glucose, 5 mmol/L HEPES, 140 mmol/L NaCl, 4 mmol/L KCl, 1 mmol/L MgCl_2 , and 1.8 mmol/L CaCl_2 , titrated to pH 7.4 with 4 mol/L NaOH. The experimental chamber held a volume of 150 μL , and the flow rate of the Tyrode's solution was 2 mL/min. Miniature solenoid valves (LFAA1201618H; Lee Products, Bucks, UK) were used to control the solution entering the chamber, and the superfusate within the chamber could be changed within 5 s. The solution level in the chamber was controlled with a suction system. The chamber and solenoid valves were mounted on the sliding stage of a microscope (Diaphot, Nikon, Japan) that sat on an antivibration table (Newport, USA).

Protease type XIV, dimethyl sulfoxide (DMSO), tetraethylammonium chloride (TEA-Cl) (all from Sigma, St Louis, MO, USA), and collagenase type 1 (Worthington Biochemical, Freehold, NJ, USA) were used in the form of stock solutions or test solutions. The H_1 antihistamine hydroxyzine and all other reagents were purchased from Sigma (St Louis, MO, USA). A stock solution of hydroxyzine was prepared in distilled water and added to the external solutions at suitable concentrations shortly before each experiment.

Membrane potential measurements were performed using conventional patch pipettes pulled from filamented thin wall glass tubing of 1.5-mm outer diameter and 1.2-mm inner diameter (World Precision Instruments, USA); when filled with 300 mmol/L KCl, the electrodes had a resistance of 25–40 M Ω . After patching onto a myocyte in the whole-cell configuration, the membrane potential was measured with an Axoclamp 900A amplifier (Axon Instruments, USA). Action potentials were elicited at 0.33 Hz by 2-ms depolarizing current pulses that were passed through the microelectrode. We selected rod shaped myocytes with clear cross striations and rejected the records with noisy or drifting baselines. Data acquisition was performed with a digital computer, analog data acquisition equipment (National Instruments, Austin, TX, USA), and the software WCP (written and supplied by John Dempster of Strathclyde University) on-line.

Expression of hERG channels in oocytes

hERG (accession No U04270) cRNA was synthesized by *in vitro* transcription of 1 μg of linearized cDNA using the mMACHINE T7 Kit (Ambion, Austin, TX, USA) and stored in 10 mmol/L Tris-HCl (pH 7.4) at -80 °C. Stage V–VI oocytes were surgically removed from female *Xenopus laevis* (Nasco, Modesto, CA, USA) that were anesthetized with 0.17% tricane methanesulfonate (Sigma, St Louis, MO, USA). Using fine forceps, the theca and follicle layers were manually removed from the oocytes, and then each oocyte was injected with 40 nL of cRNA (0.1–0.5 $\mu\text{g}/\mu\text{L}$). The injected oocytes were maintained in modified Barth's solution containing (in mmol/L): 88 NaCl, 1 KCl, 0.4 CaCl_2 , 0.33 $\text{Ca}(\text{NO}_3)_2$, 1 MgSO_4 , 2.4 NaHCO_3 , 10 HEPES (pH 7.4), and 50 $\mu\text{g}/\text{mL}$ gentami-

cin sulfate. The currents were measured two to seven days after injection. These experiments were conducted with the approval of the Research Guidelines of Kangwon National University IACUC.

Solutions and voltage clamp recordings from oocytes

Normal Ringer's solution contained 96 mmol/L NaCl, 2 mmol/L KCl, 1.8 mmol/L CaCl₂, 1 mmol/L MgCl₂, and 10 mmol/L HEPES (pH adjusted to 7.4 with NaOH). The antihistamine drug hydroxyzine and all reagents were purchased from Sigma (St Louis, MO, USA). A stock solution of hydroxyzine was prepared in distilled water and added to the external solutions at suitable concentrations shortly before each experiment. The solutions were applied to the oocytes by continuous perfusion of the recording chamber. Solution exchanges were completed within 3 min, and the hERG currents were recorded 5 min after the solution exchange. The effects of several concentrations of hydroxyzine on the hERG current were measured, and the effects were fully reversible by washing with normal Ringer's Solution. In general, each oocyte was treated with four to seven concentrations of hydroxyzine. The currents were measured at room temperature (20–23 °C) with a two-microelectrode voltage-clamp amplifier (Warner Instruments, Hamden, CT, USA). The electrodes were filled with 3 mol/L KCl and had a resistance of 2–4 MΩ for the voltage-recording electrodes and 0.6–1 MΩ for the current-passing electrodes. Stimulation and data acquisition were controlled with an AD-DA converter (Digidata 1200, Axon Instruments) and pCLAMP software (v 5.1, Axon Instruments).

Pulse protocols and analysis

To obtain concentration-response curves in the presence of hydroxyzine, dose-dependent inhibition was fitted with the equation:

$$I_{\text{tail}} = I_{\text{tail-max}} / [1 + (IC_{50}/D)^n],$$

where I_{tail} indicates the peak tail current, $I_{\text{tail-max}}$ is the maximum peak tail current, D is the concentration of hydroxyzine, n is the Hill coefficient, and IC_{50} is the concentration at which the half-maximal peak tail currents were inhibited.

HEK cell culture and transfection

HEK293 cells stably expressing HERG channels, a kind gift from Dr C JANUARY, were used for electrophysiological recordings^[13]. The method for establishing HERG channel expression in HEK293 cells is briefly described as follows. HERG cDNA was cloned into the plasmid expression vector pCDNA3 vector (Invitrogen Corporation, San Diego, CA, USA). HEK293 cells were stably transfected with HERG cDNA using a calcium phosphate precipitate method (Invitrogen) or Lipofectamine (Invitrogen). The transfected cells were cultured in minimum essential medium (MEM) supplemented with 10% fetal bovine serum, 1 mmol/L sodium pyruvate, 0.1 mmol/L non-essential amino acid solution, 100 units/mL penicillin, and 100 µg/mL streptomycin sulfate. The cultures were passaged every 4–5 d with a brief trypsin-EDTA treat-

ment followed by seeding onto 12-mm diameter glass coverslips (Fisher Scientific, Pittsburgh, PA, USA) in a Petri dish. After 12–24 h, the cell-attached coverslips were used for electrophysiological recordings.

Electrophysiology of HEK cells

HERG currents were recorded from HEK293 cells using the whole-cell patch-clamp technique at room temperature (22–23 °C)^[14]. The patch pipettes were fabricated from glass capillary pipettes (PG10165-4; World Precision Instruments, Sarasota, FL, USA) with a double-stage vertical puller (PC-10; Narishige, Tokyo) and had a tip resistance of 2–3 MΩ when filled with the pipette solution. Whole-cell currents were amplified with an Axopatch 1D amplifier (Molecular Devices, Sunnyvale, CA, USA), digitized with a Digidata 1200A (Molecular Devices) at 5 kHz and low-pass filtered with a four-pole Bessel filter at 2 kHz. Capacitive currents were canceled and series resistance was compensated by 80% with the amplifier, and leak subtraction was not applied. The generation of voltage commands and the acquisition of data were controlled with pClamp 6.05 software (Molecular Devices) running on an IBM-compatible Pentium computer. The recording chamber (RC-13, Warner Instruments Corporation, Hamden, CT, USA) was continuously perfused with bath solution (see below for composition) at a rate of 1 mL/min.

The external solution contained 137 mmol/L NaCl, 4 mmol/L KCl, 1.8 mmol/L CaCl₂, 1 mmol/L MgCl₂, 10 mmol/L glucose and 10 mmol/L HEPES (adjusted to pH 7.4 with NaOH). The intracellular solution contained 130 mmol/L KCl, 1 mmol/L MgCl₂, 5 mmol/L EGTA, 5 mmol/L MgATP and 10 mmol/L HEPES (adjusted to pH 7.4 with KOH). Hydroxyzine (Sigma Chemical Co, St Louis, MO, USA) was dissolved in distilled water at 100 mmol/L and further diluted into the bath solution.

Virtual docking

A homology model of the hERG potassium channel was built on the basis of the 1.7-Å crystal structure (PDB ID code: 1R3J) of the KvAP channel^[15] using the homology modeling program MODELLER v8.0^[16]. A 25-residue stretch of amino acids (M579 to G603) in the third extracellular loop of the hERG channel was not included in the model because this region was not present in the template structure and does not appear to be involved in the drug-induced inhibition of the hERG channel. The 3D energy-minimized conformation of hydroxyzine was generated using LigPrep version 2.0 (Schrödinger LLC, New York, NY). In the LigPrep operation, the ionization state was calculated at pH 7.4 without additional generation of the tautomer forms. The virtual docking of hydroxyzine was performed using GLIDE version 4.0 (Schrödinger LLC, New York, NY)^[17]. The extra-precision (XP) mode of GLIDE was used to achieve an accurate pose prediction. The GLIDE XP mode utilizes an improved scoring function, including a water desolvation energy term and protein-ligand structural motifs that result in enhanced binding affinity^[18]. For docking, the receptor structures were preprocessed using protein refinement

components in the GLIDE docking package. A restrained minimization using the OPLS-AA force field was performed for the refinement of the hERG channel structure. This minimization continued until the average RMS deviation of the non-hydrogen atoms reached the specified limit of 0.3 Å. To assign the candidate docking site, a grid center was defined as a centroid of the Y652 and F656 residues in the four monomers that comprised the whole hERG homology model. The grid box size was set to 15 Å from the grid center. The PoseView program (BioSolveIT GmbH, Sankt Augustin, Germany) was used to investigate the interactions of the hydroxyzine molecule with the HERG channel. All structural figures were prepared using PyMOL v1.2 (DeLano Scientific LLC, San Francisco, CA) and ChemDraw Ultra 11.0 (CambridgeSoft, Cambridge, MA).

Statistical analysis

All summary data are expressed as means±SEM. Unpaired or paired Student's *t* tests or ANOVA were used for statistical comparisons as appropriate, and differences were considered significant at $P < 0.05$.

Results

The effects of hydroxyzine on action potentials in guinea pig ventricular myocytes

In this study we examined the effects of hydroxyzine on action potentials in guinea pig ventricular myocytes. The control action potential duration at 90% (APD_{90}) of myocytes was 576 ± 45 ms ($n=9$). Figure 1A shows superimposed traces of the action potentials recorded before and during exposure to hydroxyzine at varying concentrations and exposure times. At 0.2 μmol/L, the hydroxyzine-induced lengthening of APD_{90} was positively correlated with application time, such that APD_{90} was longer after exposure for 10 min than after 5 min. This effect was more pronounced with 2 μmol/L hydroxyzine, which exerted its maximum effect on APD_{90} within 5 min. Therefore, hydroxyzine increases APD_{90} in both concentration- and time-dependent manners.

Concentration-dependence of WT hERG channel block by hydroxyzine in *Xenopus* oocytes

We next examined the effect of hydroxyzine on hERG currents using the *Xenopus* oocyte expression system. Throughout these experiments, the holding potential was maintained at -70 mV, and tail currents (I_{tail}) were recorded at -60 mV following step depolarizing pulses from -50 through +40 mV. Figure 2 shows an example of a voltage-clamp recording of a *Xenopus* oocyte and the representative current traces both under control conditions and after exposure to 5 μmol/L hydroxyzine. The amplitude of the outward currents measured near the end of the pulse (I_{HERG}) increased with increasingly positive voltage steps and reached maximum amplitude at -10 mV (Figure 3A). The I_{HERG} amplitude was normalized to the maximum I_{HERG} amplitude under control conditions and plotted against the membrane potential during the step depolarization ($I_{HERG, norm}$; Figure 3B). Increasing concentrations of hydroxyzine caused increasing inhibition of $I_{HERG, (Norm)}$, which is consistent with a

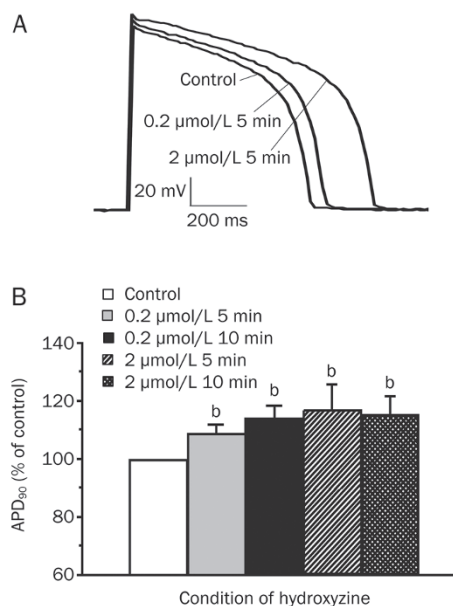


Figure 1. The effect of hydroxyzine on action potentials in isolated guinea pig ventricular myocytes. (A) Superimposed action potentials recorded before and after exposure to various concentrations of hydroxyzine. (B) Concentration- and time-dependent prolongation of action potential duration at 90% (APD_{90}). At each experimental condition (after exposure to 0.2 μmol/L for 5 min, 0.2 μmol/L for 10 min, 2 μmol/L for 5 min, and 2 μmol/L for 10 min), the APD_{90} values were normalized to control APD_{90} (obtained in the absence of drug). ^b $P < 0.05$. $n=4-9$.

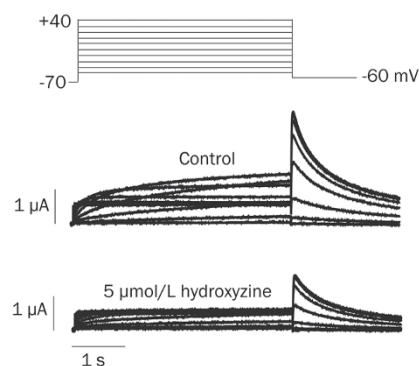


Figure 2. The effect of hydroxyzine on human *ether-a-go-go*-related gene (hERG) currents (I_{HERG}) elicited by depolarizing voltage pulses in *Xenopus* oocytes. Superimposed current traces elicited by depolarizing voltage pulses (4 s) in 10 mV increments from a holding potential of -70 mV (upper panel) in the absence of hydroxyzine (control, center panel) and presence of 5 μmol/L hydroxyzine (lower panel).

concentration-dependent effect.

After the depolarizing step, repolarization to -60 mV elicited an outward I_{tail} with an amplitude that was even larger than that of I_{HERG} during depolarization, which is due to rapid recovery from inactivation coupled with a slow deactivation mechanism^[13, 19]. When 5 μmol/L hydroxyzine was added to the perfusate, both I_{HERG} and I_{tail} were reduced (Figure 2).

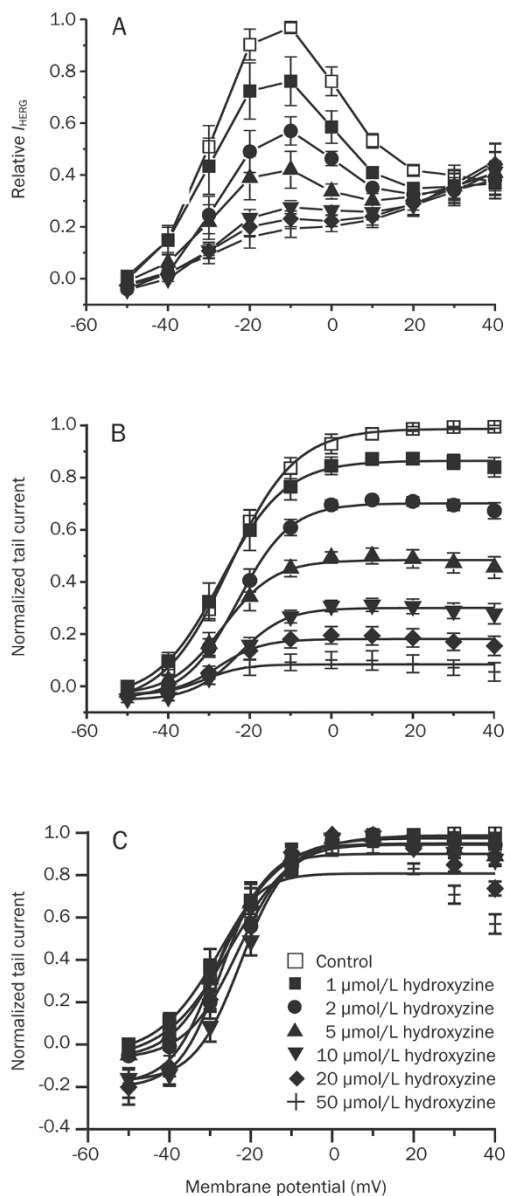


Figure 3. The effect of hydroxyzine on hERG channels expressed in *Xenopus* oocytes. (A) Plot of the normalized hERG current measured at the end of the depolarizing pulse (I_{HERG}) against pulse potential in control and hydroxyzine conditions. The maximal amplitude of the I_{HERG} in control solution was normalized to 1. (B) Plot of the normalized tail current measured at its peak following repolarization. The peak amplitude of the tail current in control solution was normalized to 1. The control data were fitted with the following Boltzmann equation, $y=1/[1+\exp\{(-V+V_{1/2})/dx\}]$, yielding a $V_{1/2}$ of -19.2 mV. (C) Activation curves with the values normalized to their respective maximum for each concentration of hydroxyzine. $n=3-5$.

The amplitude of I_{tail} was normalized to the peak amplitude obtained under control conditions at maximum depolarization and plotted against the membrane potential during the step depolarization (Figure 3B). The data obtained under control conditions were well fitted by a Boltzmann equation

with half-maximal activation ($V_{1/2}$) at -19.2 mV. The peak I_{tail} amplitude decreased with increasing hydroxyzine concentrations, indicating that the conductance of the hERG channels was decreased by hydroxyzine. In addition, in the presence of hydroxyzine, I_{tail} did not reach a steady-state level but continued to decrease at increasingly positive potentials, indicating that the blockade is more pronounced at more positive potentials.

The data presented in Figure 3B were normalized to their respective maximum values at each concentration of hydroxyzine to determine whether hydroxyzine shifts activation of hERG channels (Figure 3C). The activation curve measured in control oocytes was similar to those of oocytes treated with 1–50 $\mu\text{mol/L}$ hydroxyzine. The $V_{1/2}$ values are consistent with this finding, yielding values of -25.0 ± 0.42 , -27.0 ± 0.59 , -22.9 ± 0.61 , -26.7 ± 0.96 , -22.7 ± 0.97 , -27.8 ± 1.71 and -31.1 ± 3.40 mV in control and 1, 2, 5, 10, 20, and 50 $\mu\text{mol/L}$ hydroxyzine-treated groups, respectively ($n=3-5$, $P>0.05$, ANOVA). Therefore, the $V_{1/2}$ values in the presence of 1–50 $\mu\text{mol/L}$ hydroxyzine were similar, indicating that hydroxyzine does not alter the voltage dependence of activation for hERG channels in this concentration range.

Hydroxyzine blocks WT hERG currents in HEK cells

The IC_{50} values of many hERG channel blockers have been shown to differ depending on whether the hERG channels are expressed in *Xenopus* oocytes or mammalian cells, an effect that is probably due to the sequestration of blockers in the large ooplasm of the oocytes^[12]. We therefore tested the effect of hydroxyzine on hERG channels expressed in HEK293 cells at 36 °C (Figure 4). As shown in Figure 4A, whole-cell currents were elicited with 4-s depolarizing steps to +20 mV from a holding potential of -80 mV, and tail currents were recorded at -60 mV for 6 s. Bath-applied hydroxyzine reduced I_{HERG} in a concentration-dependent manner. The dose-dependent inhibition of the steady-state current measured at the end of a pulse to +20 mV and the peak tail current were analyzed quantitatively (Figure 4B). A nonlinear least-squares fit of dose-response plots with the Hill equation yielded an IC_{50} and Hill coefficient of 0.18 ± 0.02 $\mu\text{mol/L}$ and 1.05 ± 0.11 ($n=5$), respectively, for the steady-state current and 0.16 ± 0.01 $\mu\text{mol/L}$ and 1.23 ± 0.12 ($n=5$), respectively, for the peak tail current. Thus, hydroxyzine is ~30-fold more effective at inhibiting hERG channels expressed in HEK293 cells than in *Xenopus* oocytes.

Voltage-dependent block of WT hERG channel by hydroxyzine

We examined the hydroxyzine-induced decrease in I_{tail} at different potentials to determine whether the effect of hydroxyzine on hERG channels in oocytes was voltage dependent (Figure 5A). Dose-response relationships were measured at -20, +10, and +40 mV. The percent inhibition of the hERG current by 5 $\mu\text{mol/L}$ hydroxyzine at these voltages was $44.0\pm 8.95\%$, $47.6\pm 4.73\%$, and $54.2\pm 4.04\%$, respectively (Figure 5B). This suggests that hydroxyzine-induced block of hERG channels progressively increases with increasing depolarization.

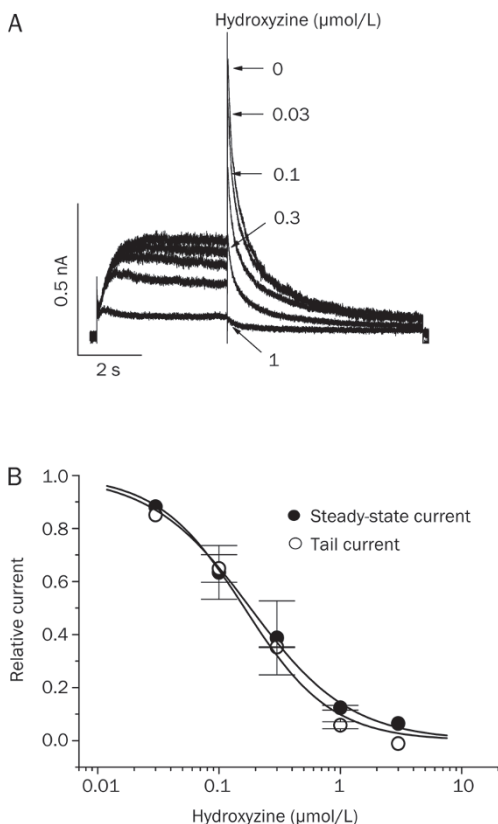


Figure 4. The concentration dependence of hydroxyzine-induced inhibition of hERG channels stably expressed in HEK293 cells. (A) Superimposed I_{hERG} traces were elicited with 4-s depolarizations to +20 mV from a holding potential of -80 mV, and the tail current was recorded at -60 mV for 6 s in the absence or presence of 0.03, 0.1, 0.3, and 1 μmol/L hydroxyzine, as indicated. The voltage protocol was applied every 15 s. The dotted line represents zero current. (B) Concentration dependence curve of inhibition by hydroxyzine for steady-state currents measured at the end of the depolarizing pulse to +20 mV or peak tail currents. The respective normalized currents were plotted against the various concentrations of hydroxyzine. The solid lines are fits of the data points using the Hill equation (see Methods).

Time-dependence of WT hERG channel block by hydroxyzine

Next we activated the current using a protocol that consisted of a single depolarizing step to 0 mV for 8 s to determine whether the channel is blocked in the closed or activated (ie, open and/or inactivated) state using the oocyte expression system (Figure 6A). After recording control currents, 5 μmol/L hydroxyzine was applied and currents were again recorded. Figure 6B shows the relative current (ie, normalized to the control current amplitude) of a representative cell. An analysis of the test pulse in the presence of hydroxyzine revealed a time-dependent block that reached 56% at 2 s (Fig-

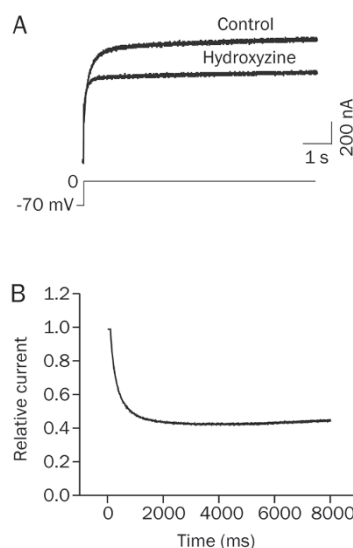


Figure 6. Relative changes in sustained hERG currents in response to hydroxyzine in *Xenopus* oocytes. (A) An example recording of currents under control conditions (control) and after application of 5 μmol/L hydroxyzine (for 7 min without any intervening test pulses). (B) Relative current obtained by dividing the current in 5 μmol/L hydroxyzine by the control current shown in in panel A. Current inhibition increased with depolarization time to 56% at 2 s in this representative cell, indicating that primarily open and/or inactivated channels were blocked.

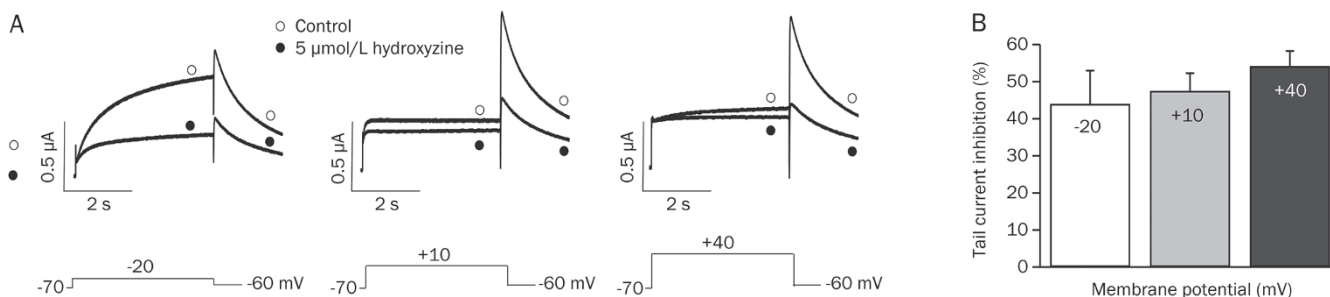


Figure 5. Voltage dependence of hydroxyzine-induced blockade of hERG channels expressed in *Xenopus* oocytes. (A) Current traces from a cell depolarized to -20 mV (left panel), +10 mV (middle panel), or +40 mV (right panel) before and after application of 5 μmol/L hydroxyzine, showing increased blockade of hERG current at more positive potentials. The protocol consisted of 4 s depolarizing steps to -20 mV, +10 mV, or +40 mV from a holding potential of -70 mV, followed by repolarization to -60 mV. (B) Hydroxyzine-induced hERG current inhibition at various voltages. At each depolarizing voltage step (-20, +10, or +40 mV), the tail currents in the presence of 5 μmol/L hydroxyzine were normalized to the tail current obtained in the absence of drug. $n=4$.

ure 6B). In contrast, at the beginning of the pulse, the normalized currents were $95\pm3\%$ of control currents ($n=4$), which indicates that the hERG channels were only slightly blocked by hydroxyzine while at the holding potential (ie, while the channels were in the closed state). In this series of experiments, $5\ \mu\text{mol/L}$ hydroxyzine reduced the hERG outward current at the end of the $0\ \text{mV}$ pulse by $48.0\pm7.2\%$ ($n=4$).

In order to address the question of whether the hERG channels are also blocked by hydroxyzine in the inactivated state, a long (4 s) test pulse to $+80\ \text{mV}$ was applied to inactivate the channels, and this was followed by a second voltage step (to $0\ \text{mV}$ for 3.5 s) to re-open the hERG channels that were not inactivated by the first test pulse; these experiments were performed in *Xenopus* oocytes ($n=3$). Figure 7A shows typical current traces under control conditions and in the presence of $5\ \mu\text{mol/L}$ hydroxyzine. Figure 7B shows the percent inhibition [ie $(1-\text{hydroxyzine current}/\text{control current})\times 100$ (in %)] upon channel opening during the second voltage pulse (to $0\ \text{mV}$), indicating that pronounced inhibition of the hERG channels had already occurred during the previous inactivating pulse to $+80\ \text{mV}$. No additional time-dependent block of the open channels was observed during the pulse to $0\ \text{mV}$. The currents at the end of the second voltage step (to $0\ \text{mV}$) were decreased by $49.1\pm12.3\%$ ($n=3$). Thus, the inhibition of hERG channels occurs primarily in the open and inactivated states but not in the closed state.

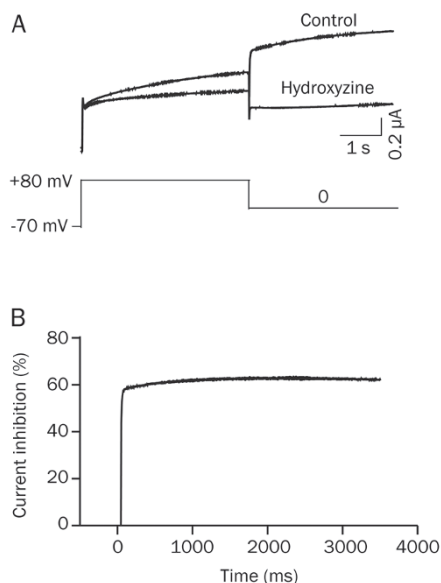


Figure 7. Blocking of inactivated hERG channels by hydroxyzine in *Xenopus* oocytes. (A) Inhibition of inactivated channels by $5\ \mu\text{mol/L}$ hydroxyzine. hERG channels were inactivated by an initial voltage-step to $+80\ \text{mV}$, followed by channel opening at $0\ \text{mV}$. (B) The corresponding relative block during the $0\ \text{mV}$ step is shown. Maximum inhibition was achieved in the inactivated state during the first step, and no additional time-dependent inhibition occurred upon channel opening during the second voltage step.

The Y652A mutation in the S6 domain attenuates hydroxyzine-mediated block of hERG channels

Tyr-652 is located in the S6 domain and faces the pore cavity of the channel, both of which are important components of the binding site for a number of compounds^[19, 20]. The potency of channel block by hydroxyzine for wild type and a mutant (Y652A) hERG channel was compared in *Xenopus* oocytes to determine whether this key residue is also important in hydroxyzine-induced block of hERG channels (Figure 8). The degree of hERG current block by $50\ \mu\text{mol/L}$ hydroxyzine was dramatically decreased by the Y652A mutation (Figure 8A). The IC_{50} values were $5.9\pm1.5\ \mu\text{mol/L}$ ($n=3$) and $35.1\pm50.5\ \mu\text{mol/L}$ ($n=4$) in WT and Y652A mutant channels, respectively (Figure 8B). This indicates that Tyr-652 is an important residue for mediating hydroxyzine-induced block of hERG channels.

Virtual docking simulation

We next performed a virtual docking simulation to elucidate

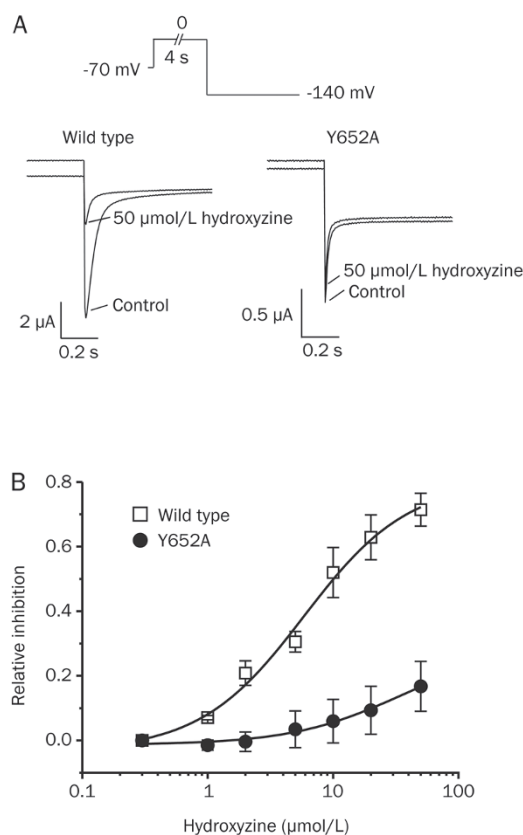


Figure 8. Concentration-dependent inhibition of WT and Y652A mutant hERG channels expressed in *Xenopus* oocytes. (A) Representative traces of WT and mutant hERG currents in the presence and absence of the indicated concentrations of hydroxyzine. The effects of the drug on WT and Y652A tail currents were recorded at $-140\ \text{mV}$ (instead of $-60\ \text{mV}$ as above) following a 4 s activating pulse. (B) The concentration-response curves were fitted with a logistic dose-response equation to yield IC_{50} values of $5.9\pm1.5\ \mu\text{mol/L}$ ($n=3$) and $35.1\pm50.5\ \mu\text{mol/L}$ ($n=4$) for WT and Y652A hERG channels, respectively.

the blocking mode of the hERG channel by hydroxyzine. Because the crystal structure of the hERG channel is not yet known, we made a homology model of the hERG channel using the K_{vAP} channel structure as the template.

The crystal structure of the K_{vAP} channel was presumably obtained in the closed state^[15]. The virtual docking was then performed by designating Tyr-652 and Phe-656 as active sites using the GLIDE program. Hydroxyzine carries a net positive charge at pH 7.4 (Figure 9A). The PoseView analysis of the highest score result showed that one of the protonated nitrogens forms a hydrogen bond with the carbonyl oxygen of Thr-623 in monomer I (Figure 9B, 9C). The etheric oxygen of hydroxyzine also makes a hydrogen bond with the hydroxyl group of Ser-649 in monomer IV. In addition to these hydrogen bonds, the aromatic group of hydroxyzine makes interactions with the side chain of aromatic rings of hERG residues Tyr-652 in monomer III and the non-aromatic side chains of Thr-623 in monomer I, Met-645 in monomer IV, Leu-646 in monomer IV and Ser-649 in monomer IV.

Discussion

Long QT syndrome can be acquired as a side effect of treatment with commonly used medications^[20]. Both cardiac and noncardiac agents cause acquired (drug induced) long QT syndrome^[21] through their inhibition of hERG channel currents^[22]. Antihistamines are widely used to treat a variety of conditions such as skin allergies, pruritus and urticaria^[7, 23]; however, some antihistamines cause QT prolongation and ventricular tachyarrhythmias^[23]. Long QT syndrome is the result of abnormal cardiac repolarization that can degenerate into ventricular fibrillation and cause sudden cardiac death^[20]. An antihistamine overdose can cause cardiac arrhythmia by directly inhibiting cardiac K^+ currents. Among the various cardiac K^+ currents, I_{Kr} is important for the termination of the cardiac action potential^[4]. The inhibition of hERG channels has been implicated in drug-induced prolongation of the QT interval and *torsades de pointes*^[24].

Hydroxyzine, a first generation H_1 -receptor antagonist, has both cardiovascular and CNS adverse effects in humans. Hydroxyzine toxicity in the CNS can manifest as generalized seizures^[9, 10]. This drug has also been implicated in cardiac adverse effects such as abnormal ventricular repolarization^[8, 9], sinus tachycardia^[9, 10] and an increased risk of dysrhythmias and sudden death^[8, 9]. In the isolated, perfused feline heart model, hydroxyzine acts directly on the heart to slow repolarization and prolong the QT interval^[8]. In our study, hydroxyzine inhibits recombinant hERG K^+ currents with an IC_{50} value of 0.16 $\mu\text{mol/L}$ in HEK cells, which is similar to the value obtained after single dose oral (0.7 mg/kg)^[25]. We also found that hydroxyzine at 0.2–2 $\mu\text{mol/L}$ prolonged APD_{90} in mammalian myocytes and inhibited hERG channels in concentration-, voltage-, time-, and state-dependent manners. Therefore, the hydroxyzine-induced cardiac adverse effects such as abnormal ventricular repolarization and increased risk of sudden death might be attributed to the drug's direct block of hERG channels, possibly by hydrogen bonds and hydrophobic

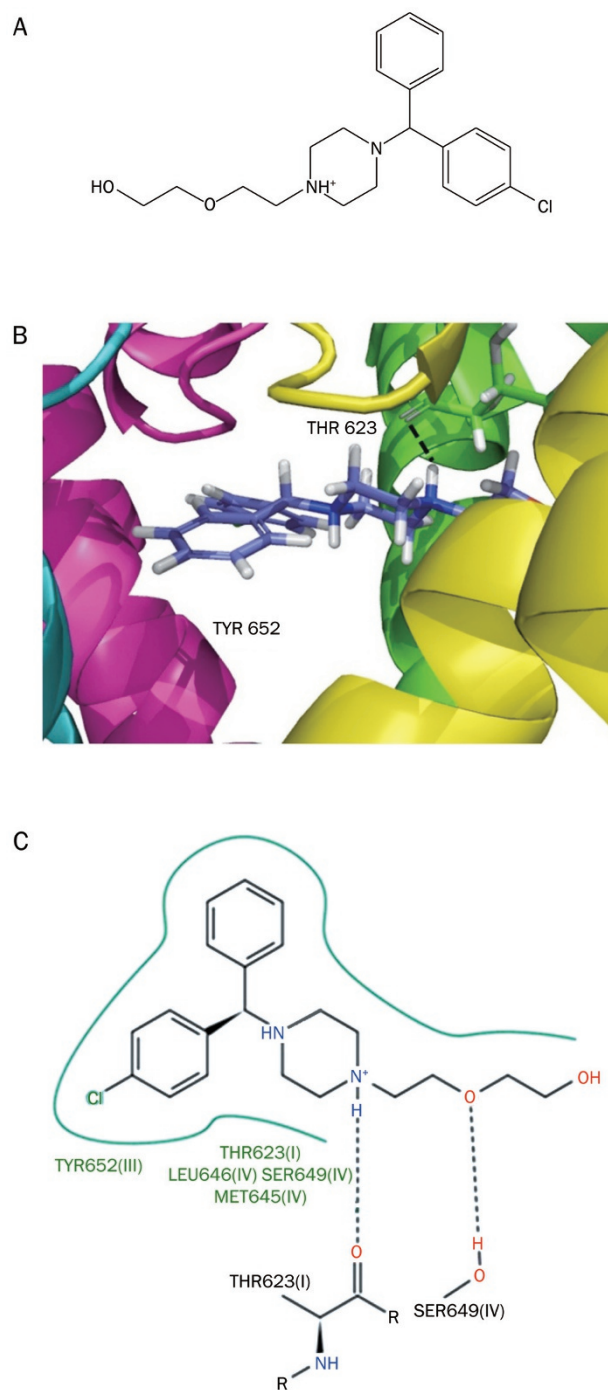


Figure 9. Docking of hydroxyzine within the inner cavity of a hERG channel homology model. (A) The major microspecies of hydroxyzine protonation at pH 7.4. (B) Inner view of hydroxyzine docked to the ligand binding site in the hERG channel. Hydroxyzine is shown in stick form and the dotted line indicates a hydrogen bond between the blocker and channel. The hERG channel inhibitor hydroxyzine shows interactions with THR623 (subunit A) and TYR652 (subunit C). (C) PoseView analysis of protein-ligand interactions. Hydrogen bonding is depicted as a dotted line between the participating atoms. The green lines with residue names and numbers indicate hydrophobic interactions between the drug and channel. Note the hydrogen bond between the hydrogen atom of the protonated nitrogen (in the hydroxyzine molecule) and the carbonyl oxygen atom of THR623(I).

interactions between the drug and the channel (Figure 9).

In the heart, the hERG gene encodes the pore-forming subunit of the rapidly activating delayed rectifier K⁺ channel (I_{Kr})^[26]. Mutations in hERG reduce I_{Kr} and cause the inherited form of type 2 long QT syndrome^[27], and the acquired long QT syndrome can occur in patients who are treated with commonly used medications^[20]. In one patient, the combination of a genetic mutation (A614V) and treatment with hydroxyzine appeared to cause severe cardiac pathophysiology that included syncope due to *torsade de pointes*^[28]. hERG channels have several putative binding sites for blocking agents^[20]. The mechanism that has been proposed for the most direct block of I_{Kr} involves the drug binding to specific amino acid residues in the pore-lining S6 region of the hERG channel^[20]. In the present study, the mutation Y652A in the S6 domain attenuated the hERG current block by about 6-fold; the IC₅₀ of hydroxyzine-dependent hERG block increased from 5.9 μmol/L to 35.1 μmol/L with the Y652A mutation (Figure 8). This result is consistent with our docking model, which shows that the aromatic group of hydroxyzine makes interactions with the side chain of aromatic rings of TYR652(III) in the hERG channel. In this context, the present study suggests that hydroxyzine is a direct and potent blocker of hERG channels and provide a molecular mechanism for the drug-induced arrhythmogenic adverse effects.

In our virtual docking simulation of the blocking mode of hERG channels by hydroxyzine, there was no interaction between the drug and F656, the amino acid that is involved in drug inhibition (Figure 9). Nonetheless, our results are consistent with our previous hERG channel blocking model in which i) a protonated nitrogen in the blocker forms a hydrogen bond with the carbonyl oxygen of residues THR623 or SER624, ii) an aromatic moiety in the blocker makes a π-π interaction with the aromatic ring of residue TYR652, and iii) a hydrophobic group in the blocker makes a hydrophobic interaction with the benzene ring of residue PHE656^[29].

In conclusion, we found that the histamine H₁-receptor antagonist hydroxyzine directly inhibits hERG channels and the I_{Kr} currents carried by these channels, thereby resulting in a prolongation of the cardiac action potential. These results help explain the mechanisms that underlie drug-induced cardiac arrhythmia.

Acknowledgements

This study was supported by a grant (08172KFDA465) from the Korea Food & Drug Administration and a grant (A100096) of the Korea Healthcare technology R&D Project, Ministry for Health, Welfare & Family Affairs, Republic of Korea.

Author contribution

Bok Hee CHOI, Han CHOE, Jin Won HYUN, and Su-Hyun JO designed the research; Byung Hoon LEE, Seung Ho LEE, Daehyun CHU, Han CHOE, and Su-Hyun JO performed the experiments; Dae-hyun CHU, Seung Ho LEE, Han CHOE, Bok Hee CHOI, and Su-hyun JO analyzed the data; Byung Hoon

LEE, Seung Ho LEE, Han CHOE, Bok Hee CHOI, and Su-Hyun JO wrote the paper.

References

- 1 Grunnet M. Repolarization of the cardiac action potential. Does an increase in repolarization capacity constitute a new anti-arrhythmic principle? *Acta Physiol (Oxf)* 2010; 198 (Suppl 676): 1–48.
- 2 Tamargo J, Caballero R, Gomez R, Valenzuela C, Delpon E. Pharmacology of cardiac potassium channels. *Cardiovasc Res* 2004; 62: 9–33.
- 3 Jo SH, Hong HK, Chong SH, Choe H. Protriptyline block of the human *ether-a-go-go*-related gene (HERG) K⁺ channel. *Life Sci* 2008; 82: 331–40.
- 4 Hong HK, Jo SH. Block of HERG K channel by classic histamine h(1) receptor antagonist chlorpheniramine. *Korean J Physiol Pharmacol* 2009; 13: 215–20.
- 5 Dennis A, Wang L, Wan X, Ficker E. hERG channel trafficking: novel targets in drug-induced long QT syndrome. *Biochem Soc Trans* 2007; 35: 1060–3.
- 6 Rajamani S, Eckhardt LL, Valdivia CR, Klemens CA, Gillman BM, Anderson CL, et al. Drug-induced long QT syndrome: hERG K⁺ channel block and disruption of protein trafficking by fluoxetine and norfluoxetine. *Br J Pharmacol* 2006; 149: 481–9.
- 7 Wong AR, Rasool AH. Hydroxyzine-induced supraventricular tachycardia in a nine-year-old child. *Singapore Med J* 2004; 45: 90–2.
- 8 Wang WX, Ebert SN, Liu XK, Chen YW, Drici MD, Woosley RL. “Conventional” antihistamines slow cardiac repolarization in isolated perfused (Langendorff) feline hearts. *J Cardiovasc Pharmacol* 1998; 32: 123–8.
- 9 Tagliatalata M, Timmerman H, Annunziato L. Cardiotoxic potential and CNS effects of first-generation antihistamines. *Trends Pharmacol Sci* 2000; 21: 52–6.
- 10 Magera BE, Betlach CJ, Sweatt AP, Derrick CW Jr. Hydroxyzine intoxication in a 13-month-old child. *Pediatrics* 1981; 67: 280–3.
- 11 Suessbrich H, Waldegger S, Lang F, Busch AE. Blockade of HERG channels expressed in *Xenopus* oocytes by the histamine receptor antagonists terfenadine and astemizole. *FEBS Lett* 1996; 385: 77–80.
- 12 Choi SY, Koh YS, Jo SH. Inhibition of human *ether-a-go-go*-related gene K⁺ channel and I_{Kr} of guinea pig cardiomyocytes by antipsychotic drug trifluoperazine. *J Pharmacol Exp Ther* 2005; 313: 888–95.
- 13 Zhou Z, Gong Q, Ye B, Fan Z, Makielski JC, Robertson GA, et al. Properties of HERG channels stably expressed in HEK 293 cells studied at physiological temperature. *Biophys J* 1998; 74: 230–41.
- 14 Hamill OP, Marty A, Neher E, Sakmann B, Sigworth FJ. Improved patch-clamp techniques for high-resolution current recording from cells and cell-free membrane patches. *Pflugers Arch* 1981; 391: 85–100.
- 15 Zhou Y, MacKinnon R. The occupancy of ions in the K⁺ selectivity filter: charge balance and coupling of ion binding to a protein conformational change underlie high conduction rates. *J Mol Biol* 2003; 333: 965–75.
- 16 Sali A, Blundell TL. Comparative protein modelling by satisfaction of spatial restraints. *J Mol Biol* 1993; 234: 779–815.
- 17 Friesner RA, Banks JL, Murphy RB, Halgren TA, Klicic JJ, Mainz DT, et al. Glide: a new approach for rapid, accurate docking and scoring. 1. Method and assessment of docking accuracy. *J Med Chem* 2004; 47: 1739–49.
- 18 Friesner RA, Murphy RB, Repasky MP, Frye LL, Greenwood JR, Halgren TA, et al. Extra precision glide: docking and scoring incorporating a

- model of hydrophobic enclosure for protein-ligand complexes. *J Med Chem* 2006; 49: 6177–96.
- 19 Sanchez-Chapula JA, Navarro-Polanco RA, Culberson C, Chen J, Sanguinetti MC. Molecular determinants of voltage-dependent human *ether-a-go-go* related gene (hERG) K⁺ channel block. *J Biol Chem* 2002; 277: 23587–95.
 - 20 Mitcheson JS, Chen J, Lin M, Culberson C, Sanguinetti MC. A structural basis for drug-induced long QT syndrome. *Proc Natl Acad Sci U S A* 2000; 97: 12329–33.
 - 21 Witche HJ, Hancox JC. Familial and acquired long QT syndrome and the cardiac rapid delayed rectifier potassium current. *Clin Exp Pharmacol Physiol* 2000; 27: 753–66.
 - 22 Taglialatela M, Castaldo P, Pannaccione A, Giorgio G, Annunziato L. Human *ether-a-go-go*-related gene (HERG) K⁺ channels as pharmacological targets: present and future implications. *Biochem Pharmacol* 1998; 55: 1741–6.
 - 23 Yap YG, Camm AJ. Potential cardiac toxicity of H1-antihistamines. *Clin Allergy Immunol* 2002; 17: 389–419.
 - 24 Roden DM. Drug-induced prolongation of the QT interval. *N Engl J Med* 2004; 350: 1013–22.
 - 25 Simons FE, Simons KJ, Frith EM. The pharmacokinetics and antihistaminic of the H1 receptor antagonist hydroxyzine. *J Allergy Clin Immunol* 1984; 73: 69–75.
 - 26 Sanguinetti MC, Jiang C, Curran ME, Keating MT. A mechanistic link between an inherited and an acquired cardiac arrhythmia: hERG encodes the I_{kr} potassium channel. *Cell* 1996; 81: 299–307.
 - 27 Keating MT, Sanguinetti MC. Molecular and cellular mechanisms of cardiac arrhythmias. *Cell* 2001; 104: 569–80.
 - 28 Sakaguchi T, Itoh H, Ding WG, Tsuji K, Nagaoka I, Oka Y, *et al*. Hydroxyzine, a first generation H(1)-receptor antagonist, inhibits human *ether-a-go-go*-related gene (HERG) current and causes syncope in a patient with the HERG mutation. *J Pharmacol Sci* 2008; 108: 462–71.
 - 29 Choe H, Nah KH, Lee SN, Lee HS, Jo SH, Leem CH, *et al*. A novel hypothesis for the binding mode of HERG channel blockers. *Biochem Biophys Res Commun* 2006; 344: 72–8.